ACS BIO & MED CHEM Au
AN OPEN ACCESS JOURNAL OF THE AMERICAN CHEMICAL SOCIETY

pubs.acs.org/biomedchemau

Article

Stable Gold-Nanoparticle-Based Vaccine for the Targeted Delivery of Tumor-Associated Glycopeptide Antigens

Kevin R. Trabbic, Kristopher A. Kleski, and Joseph J. Barchi, Jr.*

Cite This: *ACS Bio Med Chem Au* 2021, 1, 31–43

Read Online

ACCESS | Metrics & More | Article Recommendations | Supporting Information

ABSTRACT: We have developed a novel antigen delivery system based on polysaccharide-coated gold nanoparticles (AuNPs) targeted to antigen-presenting cells (APCs) expressing Dectin-1. AuNPs were synthesized de novo using yeast-derived β-1,3-glucans (B13G) as the reductant and passivating agent in a microwave-catalyzed procedure, yielding highly uniform and serum-stable particles. These were further functionalized with both a peptide and a specific glycosylated form from the tandem repeat sequence of mucin 4 (MUC4), a glycoprotein overexpressed in pancreatic tumors. The glycosylated sequence contained the Thomsen−Friedenreich disaccharide, a pan-carcinoma, tumor-associated carbohydrate antigen (TACA), which has been a traditional target for antitumor vaccine design. These motifs were prepared with a cathepsin B protease cleavage site (Gly-Phe-Leu-Gly), loaded on the B13G-coated particles, and these constructs were examined for Dectin-1 binding, APC processing, and presentation in a model in vitro system and for immune responses in mice. We showed that these particles elicit strong in vivo immune responses through the production of both high-titer antibodies and priming of antigen-recognizing T-cells. Further examination showed that a favorable antitumor balance of expressed cytokines was generated, with limited expression of immunosuppressive Il-10. This system is modular in that any range of antigens can be conjugated to our particles and efficiently delivered to APCs expressing Dectin-1.

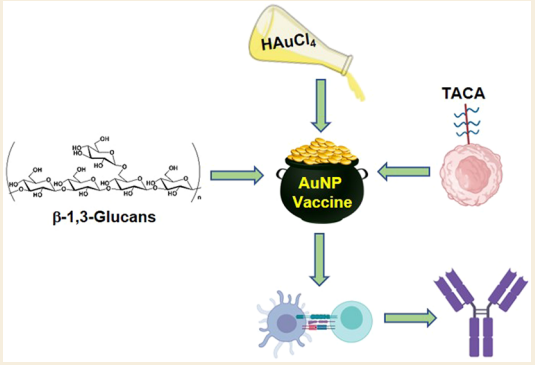

KEYWORDS: *glycopeptides, Thomsen−Friedenreich antigen, vaccine, β-1,3-glucans, antigen-presenting cells, Dectin-1, immunogens, T-cells*

INTRODUCTION

Tumor-associated carbohydrate antigens (TACAs) are glycan structures covalently attached to proteins or lipids in various forms on the surface of tumor cells.[1−3] They differ from the normal cell glycan repertoire insofar as the tumor biosynthetic machinery is modified via a disparate regulation of glycosyltransferases and hydrolases. This produces aberrant and distinct cell-surface glycan structures that are unique to tumors, and these structures impart modified biophysical and protein-binding characteristics to individual tumor types. In addition, some of these tumor-associated glycans can be recognized as "nonself" by the immune system (hence the moniker, "antigen"), eliciting both humoral and (sometimes) cell-mediated responses.[4] As a result, there have been myriad attempts to prepare vaccine constructs to raise effective and durable immune responses to TACAs.[5−14]

The immune response to TACAs notwithstanding, they are composed of self-molecules and hence are innately weak immunogens on their own. Carbohydrates are also T-cell-independent epitopes, and mobilization of that arm of the immune response is essential to eradicate any established tumor.[11] It is thus not surprising that vaccine development against these antigens has been problematic; however, many strategies have met with success. The use of various delivery platforms,[5,15−18] conjugations to immunogenic proteins (KLH, tetanus toxin)[19] or peptide epitopes to generate T-cell help,[20−23] covalent conjugation to Toll-like receptor agonists,[7,19,21,24] the use of various adjuvants[25] and attachment to zwitterionic polysaccharides[4,26] have led to robust immune responses to carbohydrate structures and some have moved into clinical trials. However, none of these efforts have led to a truly effective, FDA-approved therapy against any type of cancer.

Research into the use of different nanomaterials for a host of medical applications has exploded in recent years, and many of these applications are for some form of targeted drug delivery to treat various ailments in animal models. It follows that some of these same materials have been purposed as vaccine platforms to deliver antigens, adjuvants, and T-cell epitopes,

Received: June 22, 2021
Published: September 10, 2021

https://doi.org/10.1021/acsbiomedchemau.1c00021
ACS Bio Med Chem Au 2021, 1, 31–43

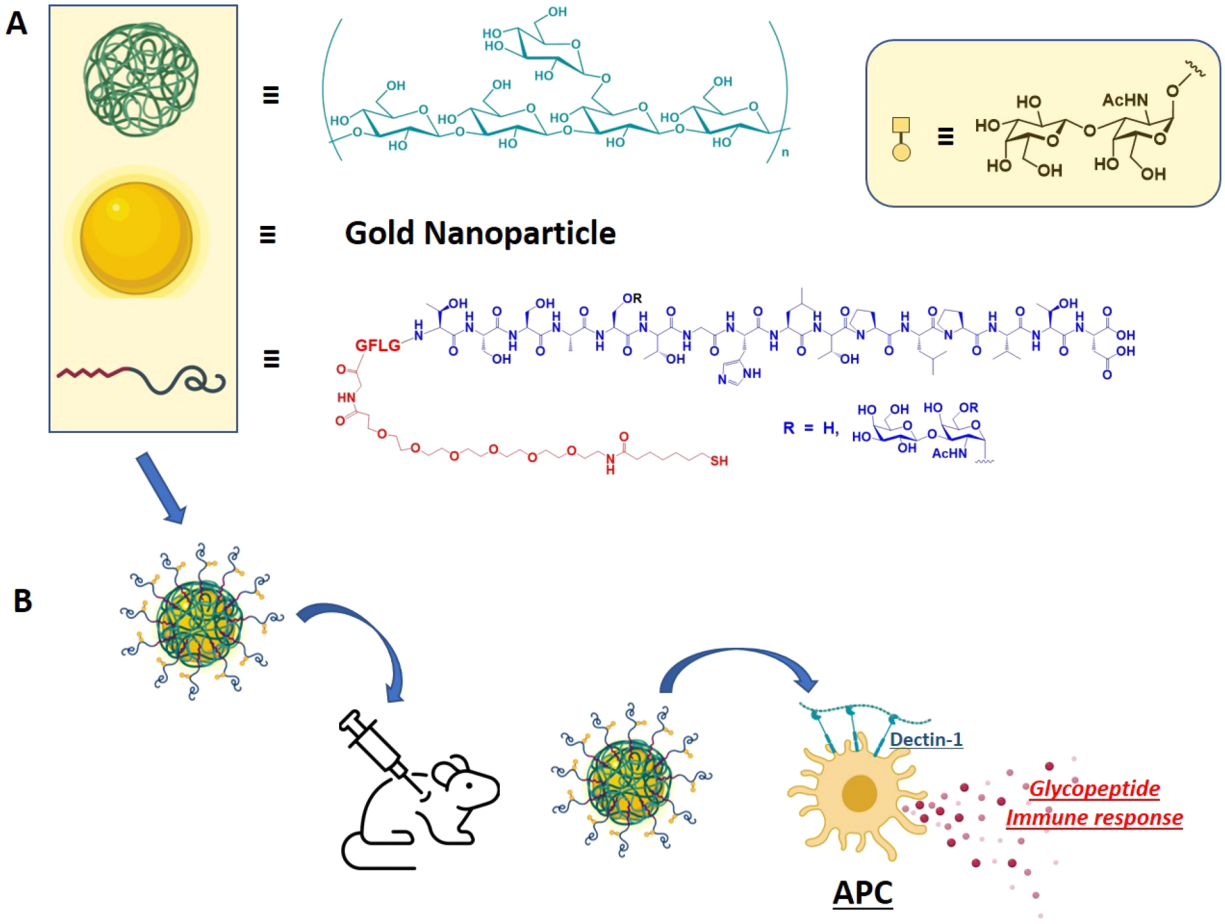

Figure 1. Schematic representation of particle components. (A) β-1,3-glucan (green), gold nanoparticle (gold), and MUC4 glycopeptide antigen (red/dark blue curved line; red = linker, blue = glycopeptide); tetrapeptide -GFLG- was inserted as a cathepsin B cleavage site. (B) Combined nanoparticle used for in vivo production of specific immune responses in mice.

either alone or in some combinations to generate functional immune responses against disease.[27] Along with applications to infectious diseases, the search for anticancer vaccines has spawned much work in this area. The list of nanomaterials employed is now quite extensive, and those include metallic nanoparticles, glycodendrimers, liposomes, and natural materials.[15,28] Some examples of TACA/nanoparticle-based platforms for cancer immunotherapy include (1) liposome and lipid-based particles,[29] (2) metallic and/or ferromagnetic particles,[30−32] (3) synthetic biodegradable polymers or hydrogels,[33] and (4) virus-like particles (VLPs).[18,34,35] Of the metallic particles, gold nanoparticles (AuNPs) have emerged as the most versatile and hence most utilized for various therapeutic applications. They can be easily synthesized in a size-selective manner and be coated with most any appropriately functionalized molecular family (proteins, small molecules, carbohydrates, lipids). These features led us to develop various AuNPs as either antitumor therapies or vaccines.[36−41] Our original vaccine platform utilized a complex mixture of a glycopeptide antigen and molecular adjuvant all coated on a gold nanoparticle where we added a spacer to reduce antigen density.[37] The glycopeptide was derived from the tandem repeat unit of a mucin protein (MUC4) that is over/aberrantly expressed on pancreatic ductal adenocarcinomas (PDACs)[42] and contained glycosylated serine or threonine residues containing the Thomsen−Friedenreich (TF) antigen, a well-known TACA presented almost exclusively on tumor tissue.[43,44] This first generation produced a moderate antibody response and identified a lead glycopeptide that had superior antitumor properties relative to other epitopes used (unpublished data). This glycopeptide, where the TF disaccharide was attached to the serine at position 5 (which we call MUC4-TF-Ser(5)), was used to raise a monoclonal antibody (mAb) that we showed to be highly PDAC-specific.[45] We sought to use this epitope in a redesigned AuNP platform that could be targeted to antigen-presenting cells (APC), such as macrophages and dendritic cells, while being versatile enough to allow further modifications with appropriate components to facilitate robust immune responses.

APCs express a wide variety of receptors on their surface that facilitate binding and uptake of foreign antigens displayed on bacteria, viruses, fungi, and tumors. These are sometime referred to as pattern recognition receptors (PRRs) as they recognize specific foreign antigens on microbes (so-called pathogen-associated molecular patterns, PAMPs) as part of the innate immune response.[46] Two categories of PRRs are the Toll-like receptors (TLRs)[47,48] and the C-type lectins (CTLs), which are calcium-dependent carbohydrate-binding proteins (CBPs).[49] These specialized proteins all recognize distinct molecular patterns, each driving various cellular signaling events that lead to cytokine production, immune cell activation, and mobilization. Both sets of receptors have been targeted to stimulate responses in antimicrobial or antitumor immunotherapy. Many CTLs have been targeted

https://doi.org/10.1021/acsbiomedchemau.1c00021
ACS Bio Med Chem Au 2021, 1, 31−43

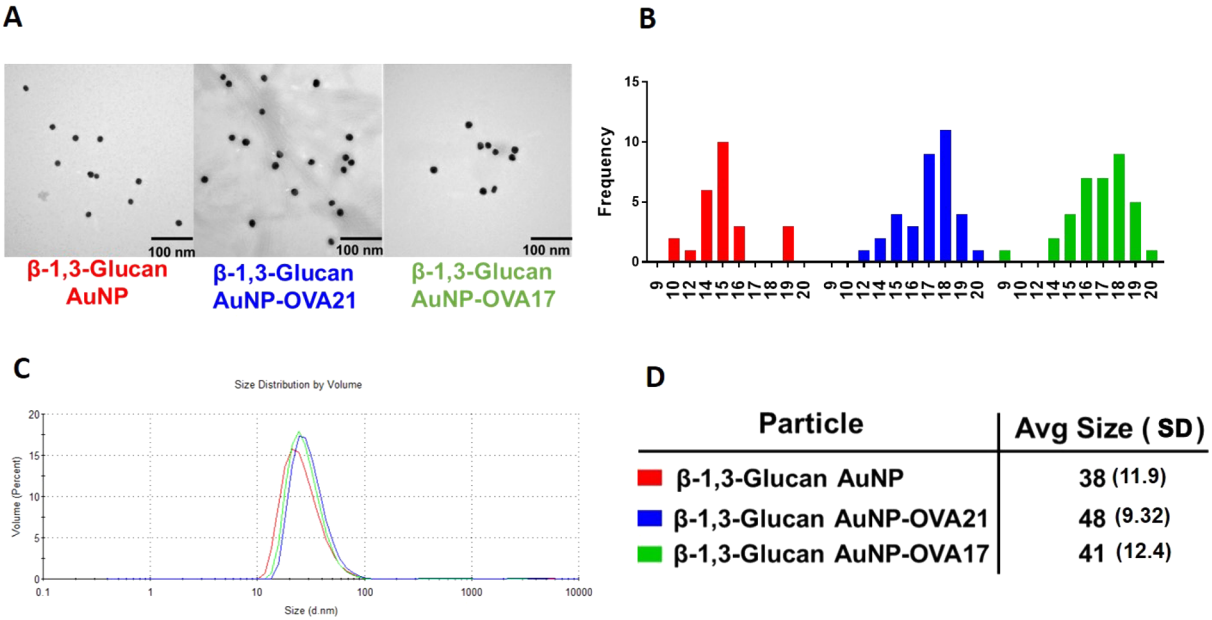

Figure 2. Representative characterization data for B13G-AuNPs and B13G-AuNPs conjugated with OVA peptides. (A) Transmission electron micrographs. (B) Size histograms for the TEM data in (A); a total of 25, 26, and 36 particles were examined for each system. (C) Dynamic light scattering volume distributions. (D) Hydrodynamic diameter (in nm) of nanoparticles determined from DLS data in (C). Average standard deviations are in parentheses.

through conjugation of their cognate carbohydrate ligands onto various platforms as therapeutic strategies against infectious diseases and cancer. Some CTLs that have been targeted include dendritic cell-specific intercellular adhesion molecule-3-grabbing nonintegrin (DC-SIGN),[16,50] the mannose receptor (MR),[16] macrophage−galactose-type C-type lectin (MGL),[51−54] and the Dectins (1, 2, and 3).[55−57] Dectin-1 is a CTL that binds β-1,3-glucans (B13G), the most abundant polysaccharide in many fungal species; this engagement initiates signaling which is mediated through an intracellular immune-receptor tyrosine-based activation motif (ITAM).[49] Tyrosine phosphorylation by Src-family kinases initiates a signaling cascade leading to NF-κB activation and the production of various inflammatory cytokines.[49] In addition, targeting Dectin-1 with B13G has been a strategy to deliver antigens to APCs, as engagement with B13G initiates endocytosis, leading to antigen presentation via MHC-II molecules.[58] B13G have been widely used as immune stimulants for their ability to kick-start the production of reactive oxygen species (ROS), inflammatory cytokines, and microbial killing. The Dectin-1/B13G signaling system has been referred to as a bridge between innate and adaptive immunity.[59]

In this work, we combined the strategy of using AuNPs as a delivery platform but designed in such a way to target Dectin-1 on APCs via B13G; this would deliver glycopeptide antigens derived from tumor-associated mucins (vide supra) in an effort to generate a glycopeptide-specific immune response. The B13G polysaccharide was used as both the reductant and the stabilizing agent to create a platform that could further be coated with antigenic sequences. There have been several studies that have prepared AuNPs in this way using various naturally derived gums and other saccharide components[60−63] as well as B13G.[64,65] However, none of these studies utilized the polysaccharide as a targeting agent. Here, we report a simple synthetic strategy toward these multifunctional AuNPs to deliver glycopeptide antigens and raise potent immune response to these antigens as measured by antibody and cytokine production.

RESULTS

We were encouraged from our previous study[37] to pursue a refined AuNP platform for a vaccine that can deliver glycopeptide antigens derived from proteins that are overexpressed in tumors and display various covalently linked TACAs. There are a variety of carriers that have been studied, many based on inorganic nanoparticles or some type of "organic" nanoconstruction, for example, from modified viruses (modified adenoviruses, bacteriophages, and virus capsid proteins). However, due to the simplicity of AuNP synthesis and manipulation, it was decided to develop a modular AuNP system that could be delivered to APCs easily and efficiently. We chose the Dectin-1/β-1,3-glucan system based on the following: (1) Dectin-1 is an atypical CLR in that is does not have a requirement for calcium,[66] and so activity would not be as sensitive to divalent metals. (2) Signaling through Dectin-1/β-1,3-glucan elicits the production of inflammatory cytokines that may skew the T-cell repertoire toward and antitumor response.[67] (3) Many polysaccharides and gums have been used to prepare AuNPs,[62,68−70] as well as B13G, but they have not been utilized for TACA-containing glycopeptide antigen delivery. A schematic representation of our overall plan is shown in Figure 1.

Peptide/Glycopeptide/Linker Synthesis

The synthesis of the various peptides and glycopeptides followed from our previous studies with slight modifications.[37,41] The linker was the same we used in our vaccine work since we had shown then and more recently[45] that this was a robust and nonimmunogenic motif to connect our antigens to nanoparticles. For this work, we used a CEM Liberty PRIME microwave peptide synthesizer to prepare all peptides. This instrument uses OxymaPure/diisopropylcarbo-

https://doi.org/10.1021/acsbiomedchemau.1c00021
ACS Bio Med Chem Au 2021, 1, 31−43

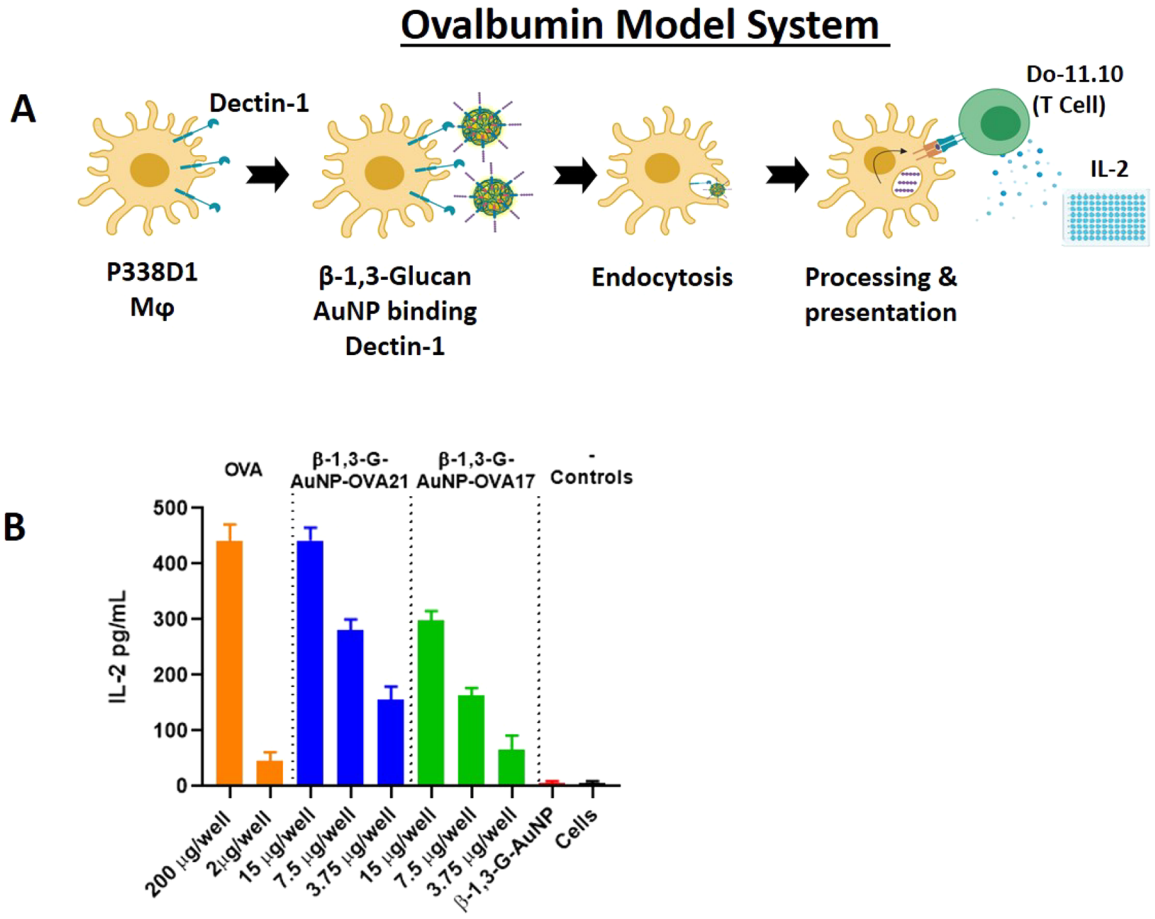

Figure 3. (A) Schematic scheme of the OVA model system. (B) Readout of IL-2 release from treatment of P338D1 macrophages with various controls and B13G-AuNPs, followed by incubation with OVA-specific T-cell clone Do-11.10.

diimide activation with 2 min peptide coupling cycles at 90 °C. Most glycoamino acid couplings were performed manually using conditions developed previously to minimize α-carbon amino acid epimerization.[71] Those performed on the Liberty PRIME instrument included an equivalent of Hunig's base (diisopropylethyl amine, DIEA) to offset the slightly acidic conditions afforded in Oxyma-activated amino acid couplings. Deprotection of the carbohydrate acetate groups was affected by treatment with 0.5 M sodium methoxide in methanol solution. All peptides were purified by reverse-phase high-performance liquid chromatography and characterized by electrospray ionization and matrix-assisted laser desorption/ionization (MALDI) mass spectrometry as well as NMR spectroscopy (see Supporting Information)

Synthesis and Characterization of B13G-Coated AuNPs

There is precedent for the *de novo* preparation of AuNPs employing the reducing end of a polysaccharide to both reduce Au^{3+} to Au^0 and simultaneously passivate the resulting particles with the oxidized polymer.[62] For other AuNP syntheses, relative concentration, temperature, and reaction conditions will dictate the size and quality of the particles. The physical characteristics of the polysaccharide offer challenges, such as solubility and issues with interconverting tertiary structures and conformations. B13G are subject to these challenges; they assume triple helix structures in solution and often need high pH to denature and hence solubilize the polymers.[72−77] Our synthesis started with the dissolution of the B13G in 4 mM NaOH solution with heating under microwave irradiation. We found that the use of microwaves facilitated the efficient and high-quality synthesis of the nanoparticles. After dissolution of the B13G in base and the addition of $HAuCl_4$, the AuNPs form smoothly in about 90 min under microwave irradiation. The synthesis and select characterization data for B13G-AuNPs and those coated with ovalbumin (OVA)-derived peptides (as part of our *in vitro* model study, *vide infra*) are shown in Figure 2. The particles are very uniform by transmission electron microscopy (TEM, Figure 2A,B) and dynamic light scattering (DLS, Figure 2 C,D), with average core diameters of 15−17 nm and hydrodynamic diameters much larger at ∼40 nm, indicative of a large and possibly highly hydrated polymer coated on the particle surface.[78] We found the procedure to be very reproducible and the batch-to-batch size measurements to be highly comparable (see Supporting Information Figures S1−S4). We performed carbohydrate analysis via a simple phenol−sulfuric acid assay to determine the total carbohydrate content on the particle. Total carbohydrate content was measured as glucose monomers and was found to be 2 mmol glucose in 50 μg/mL of AuNP (Figure S5). Zeta-potential measurements showed that the B13G-AuNPs showed an average of −35.2 mV, which was reduced to average charges of −21 mV upon conjugation of MUC4 peptide or TF-MUC4 glycopeptide via place exchange reactions. Based on the displacement of B13G upon peptide/glycopeptide conjugation, a trend toward more positive potential is consistent with removal of some B13G during immunogen conjugation (see subsequent sections). The absolute value between −21 and

https://doi.org/10.1021/acsbiomedchemau.1c00021
ACS Bio Med Chem Au 2021, 1, 31−43

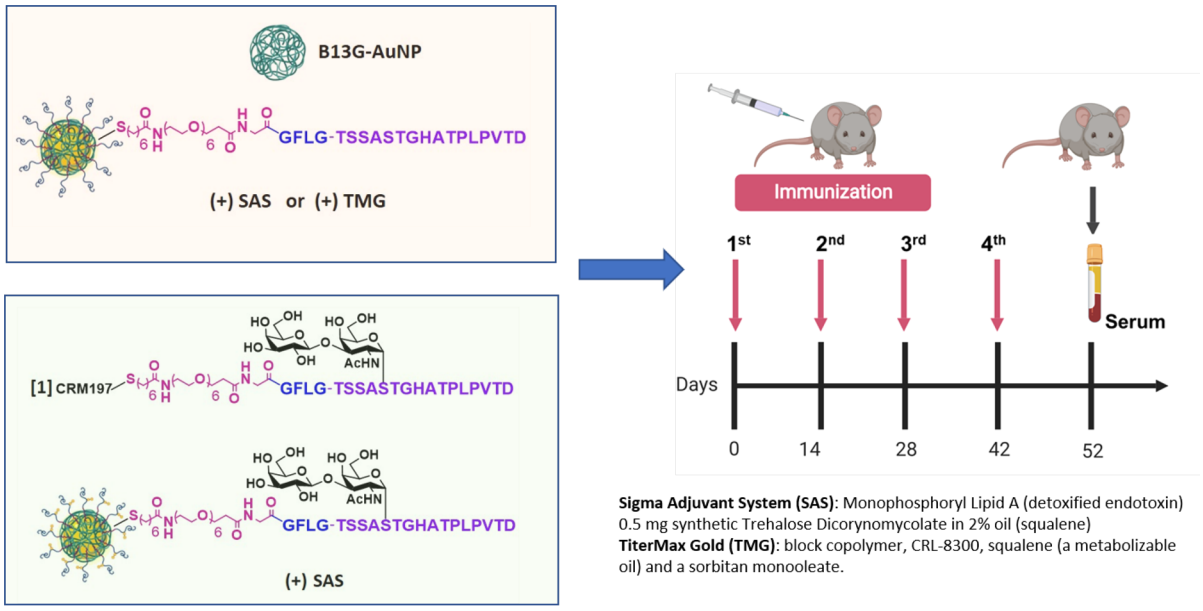

Figure 4. Protocol for *in vivo* immunizations. In stage 1 (pink box), animals were injected with either B13G-AuNPs or MUC4-B13G-AuNPs with either the Sigma Adjuvant System or TiterMax Gold as adjuvants (descriptions on lower right) with immunization schedule shown on the right, with serum collected at day 52. In stage 2 (light green box), the glycopeptide-coated particles, TF-MUC4-B13G-AuNPs were injected with SAS or with CRM197-TF-MUC4 conjugate (no nanoparticles). Each stage contained a control group of mice injected with PBS.

−35 also suggests the particles should remain stable in solution and avoid aggregation.[79]

Conjugation of Peptide/Glycopeptide Sequences to B13G-Coated AuNPs and Estimation of Peptide Coverage

The attachment of the peptide antigens to our newly synthesized B13G-AuNPs was performed by a simple place exchange reaction with our thiol-containing linked constructs. We were initially unsure if this would be successful considering the probable high coverage of the gold surface by the glycan polymer. However, coating with peptides or glycopeptides went smoothly as we were able to confirm the addition of these antigens by several indirect methods. As described above, for the unconjugated particle, we performed carbohydrate analysis postconjugation to observe any displacement of the polymer. The results from this analysis suggested an approximate 50% drop in carbohydrate concentration after addition of the antigens, suggesting a displacement of polymer from the gold surface. This is expected as the polymer coating is through noncovalent interaction interactions in contrast to the stronger dative-type bond (~40 kcal/mol)[80] formed between thiol and gold when antigen is conjugated.

Estimates of the peptide coverage was qualitatively made by the displacement of a fluorescent thiolated peptide that was conjugated to the B13G-coated particles. For this, we used a commercially available 5 kDa FITC-PEG thiol that we conjugated to the B13G-AuNP. This in turn displaced a portion of the B13G from the particle, while the attachment caused the well-known fluorophore quenching by the Förster resonance energy transfer properties of three-dimensional self-assembled monolayers of gold. Subsequent release of the PEG fluorophore by treatment with dithiothreitol restored fluorescence, which was quantitated at 525 nm. This corresponded to a loading of 362 nM FITC-PEG per a solution of 400 μg/mL of nanoparticle (Figure S6).

Dectin-1 Binding

The B13G-AuNPs were compared with free B13G for binding to Dectin-1. As shown in Figure S7, ELISA assays where the polysaccharide was bound to the wells and binding was analyzed with Fc-Dectin-1 (InvivoGen, Ca) demonstrate that B13G-AuNPs bind equally well or better than soluble B13G in a dose-dependent manner. Binding was observable down to single digit nanomolar concentrations. This result showed that the binding to the targeted C-type lectin was recapitulated in the designed B13G-stabilized particles.

Vaccination Studies with B13G-AuNPs: In Vitro Model Study with OVA Peptides

Before attempting any *in vivo* experiments, initial evaluation of the B13G-AuNPs with a model system was performed as an in vitro prescreen for appropriate biological activity. Our design took advantage of the availability of a macrophage/T-cell clone pair that can present and recognize a specific ovalbumin peptide, respectively. Tumor macrophage Dectin-1-expressing cell line P388D1 was paired with the Do-11.10 T-cell clone, which expresses a T-cell receptor that recognizes a specific 17 amino acid ovalbumin MHC class-II epitope. In brief, uptake and presentation of the OVA peptide by P388D1 cells within the context of MHC-II will allow recognition by the T-cell clone and release of IL-2. We synthesized this 17 residue peptide encompassing the recognition domain containing OVA amino acids 324−340 (i.e., in single amino acid code: ISQAVHAAHAEINEAGR) and coupled the N-terminus to our thiol-containing linker (OVA17) for conjugation to B13G-AuNPs (see Figure 3A for a description of the experiment). We also synthesized a second peptide containing a tetrapeptide cathepsin B protease recognition domain (-GFLG-) after the N-terminal isoleucine and directly before linker attachment (OVA 21). Cathepsins are proteases known to facilitate endosomal antigen processing after receptor-mediated uptake into APCs. The peptides were characterized by NMR and both ESI and MALDI mass spectrometry (see Supporting

https://doi.org/10.1021/acsbiomedchemau.1c00021
ACS Bio Med Chem Au 2021, 1, 31−43

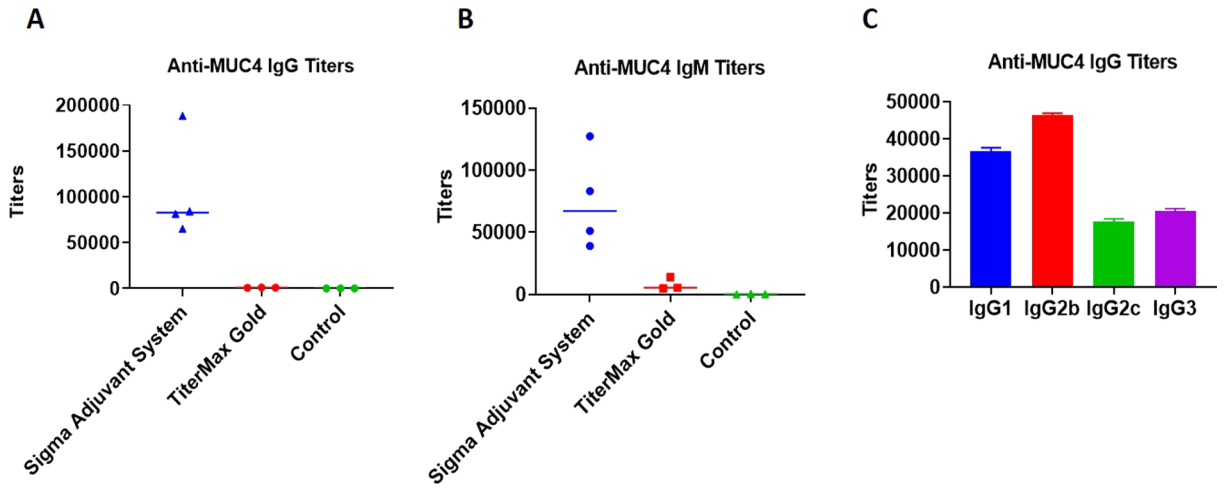

Figure 5. Graph of antibody titers to the MUC4 21-mer peptide from stage 1 immunizations: (A) IgG, (B) IgM, and (C) IgG subtypes.

Information for all characterization data). Each of these was coupled to B13G-AuNPs as described above. Figure 3 shows the IL-2 readout resulting from incubation of the OVA-conjugated B13G-AuNPs with both the P388D1 and Do-11.10 cells as described in Experimental Section. As shown in Figure 3B, in a 15 μg well, the B13G-OVA21-AuNP construct was as active as the peptide alone at 200 μg/well (positive control), while the construct without the cathepsin cleavage motif (B13G-OVA17-AuNP) was about half as active as the OVA21 construct. These results suggested that the particles function to enter Dectin-1-expressing APCs and retain the ability to present peptide (glycopeptide) cargo to T-cells.

In Vivo Vaccination Studies with B13G-MUC4/Glycopeptide-Loaded AuNPs

Based on the ovalbumin study, we prepared B13G-AuNPs with our MUC4 peptide/glycopeptides from Figure 1. These studies were performed in two stages. First, we prepared B13G-AuNPs conjugated with the unglycosylated MUC4 peptide (B13G-MUC4-AuNPs) and immunized with two distinct adjuvants to determine the most efficient combination for immune enhancement. Second, the TF-Ser(5) glycopeptide was conjugated to B13G-AuNPs (B13G-TF-Ser(5)-MUC4-AuNPs) utilizing the adjuvant chosen in the first vaccination. In this step, the glycopeptide was also conjugated to the highly immune-stimulating protein carrier CRM197 (B13G-TF-Ser(5)-MUC4-CRM197), a recombinant, nontoxic form of diptheria toxin used as a carrier protein for many polysaccharides[81−83] as a "positive" control. This was done to compare the new platform to one known to elicit very powerful immune responses to many different haptens. All synthetic haptens were prepared with the -GFLG- tetrapeptide cathepsin B cleavage site based on the superior performance of these constructs in the model study. See Figure 4 for a general description of the experimental protocol.

Each stage consisted of groups of five mice to be injected. Stage 1 consisted of four groups: (A) those inoculated with B13G-AuNPs (negative control), (B) two groups immunized with B13G-MUC4-AuNPs, one for each of two adjuvants, and (C) PBS. The experimental design is summarized in Figure 4. The two separate adjuvants were (1) the Sigma Adjuvant System (SAS), which consists of monophosphoryl lipid A (a detoxified endotoxin) and synthetic trehalose dicorynomycolate in a 2% squalene oil base, and (2) TiterMax Gold (TMG), which is a mixture of a block copolymer (CRL-8300) and sorbitan monooleate, also in a squalene base. Interestingly, only immunization with SAS elicited both humoral (Figure 5A−C) and cell-based immune responses. Both IgG and IgM titers against the MUC4 epitope were generated, with values as high as 180,000 for the IgG isotype. The IgGs generated were primarily of the IgG1 and IgG2b subtypes. Control particles gave no response, and the TMG vaccination only showed very low IgM titers of any immunoglobulin type.

The SAS vaccine subgroup was analyzed by a cytokine bead assay. The repertoire of cytokines expressed can be used as a measure of a cell-mediated response and to stratify the T-helper subtypes that were generated. The SAS adjuvant subset showed stimulation of IL-1β, IL-5, IL-6, IFN-γ, IL-17, IL-21, IL-23, and MIP3α. Only IL-6 and IL-10 production was seen in the TMG subset from this pilot study, indicating a more immmunosuppressive environment in these mice (see Figures S8−S11). Due to this undesirable outcome and the overall low levels of cytokines expressed in the TMG-adjuvanted mice, it was decided to use only SAS in the follow-up trial with the TF-Ser(5)-MUC4 glycopeptide and any other subsequent vaccination trial with glycopeptide antigens.

Stage 2 also consisted of four groups: a PBS group and a B13G-AuNP group similar to stage 1, a B13G-TF-Ser(5)-MUC4-AuNPs group, and one group vaccinated with a TF-Ser(5)-MUC4-CRM197 conjugate (formed by coupling the thiolated antigen to CRM197-maleimide, purchased from Fina Biosolutions, LLC; see Figure S12 for a MALDI mass spectrum of the conjugate). The stage 2 study proceeded identically to the MUC4 peptide study in terms of immunization frequency and amounts of nanoparticles injected, and all of the vaccinations were performed with the SAS adjuvant (vide supra). The CRM197 conjugate generated a very intense immune response with antibody titers as high as 800,000 (Figure S13). Our B13G-TF-Ser(5)-MUC4-AuNPs also generated very respectable immunoglobulin responses, comparable to those seen with the unglycosylated peptide nanoparticles (IgG titers as high as 300,000). These results suggested that the platform we are using can generate high humoral immune responses without the need for highly immunogenic carrier protein (see Discussion).

The cell-mediated response from vaccinations with the B13G-TF-Ser(5)-MUC4-AuNPs was also comparable to the response seen from animals vaccinated with unglycosylated

https://doi.org/10.1021/acsbiomedchemau.1c00021
ACS Bio Med Chem Au 2021, 1, 31−43

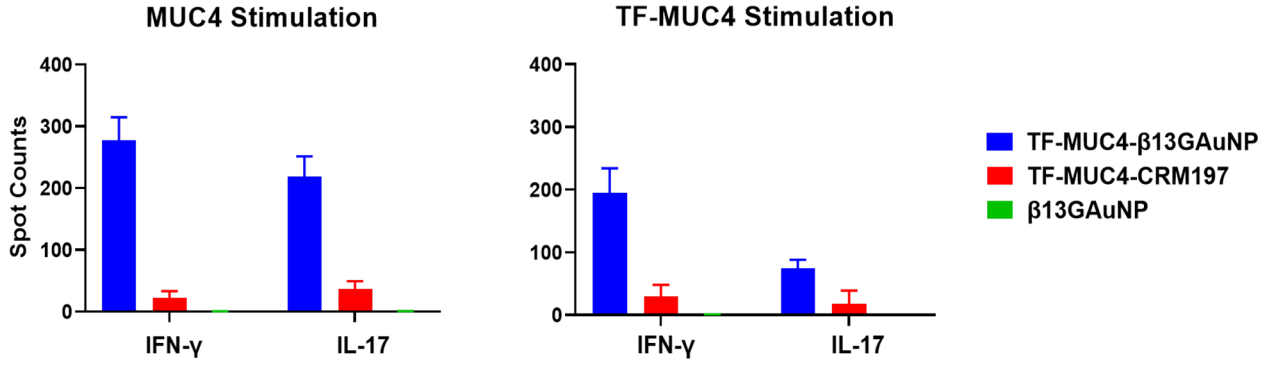

Figure 6. Graphs of ELISpot disk counts comparing vaccinations of our TF-Ser(5)-MUC4-B13G-AuNP conjugate the TF-Ser(5)-MUC4-CRM197 conjugate and control B13G-AuNPs when panned for interferon-γ and IL-17 production. While the TF-Ser(5)-MUC4-CRM197 conjugate has an intense humoral response, the TF-MUC4 vaccine construct elicited a much stronger $CD4^+$ T-cell response, whereas the control B13G-AuNPs consistently showed no response.

peptide-conjugated B13G-AuNPs. While the Th2 response was similar between glycopeptide or peptide-based vaccines, the IFN-γ quantities were about 2-fold higher in the glycopeptide-vaccinated animals. ELISpot analysis of splenocytes isolated from sacrificed animals (see Figure S14) showed proliferation of both peptide and glycopeptide-specific T-cell clones, all suggesting that antigen-conjugated B13G-AuNPs can be taken up by APCs and their cargo presented to T-cells (Figure 6). Important to both vaccination studies was the absence of Il-10 protein expression elicited by either of our vaccines. IL-10 is a cytokine that suppresses the ability of DCs to stimulate $CD4^+$ T-cell proliferation and reduces IFN-γ production.[84,85] In addition, only the CRM197 conjugate sera contained TGF-β, another cytokine that can have both immunosuppressive and antiapoptotic effects. Importantly, a trial of the pancreatic cancer vaccine GVAX showed potentiated antitumor activity when combined with TGF-β blockade.[86]

DISCUSSION

In this study, we have prepared a AuNP that combines an APC-targeting moiety and a novel glycopeptide antigen. This antigen was chosen since we had previously shown that an antibody raised to this glycopeptide was tumor-specific.[45] The use of B13G polymers as both stabilizing and targeting agents has produced a nanoparticle that is adaptable and multifunctional. The microwave-assisted synthesis of the B13G-AuNPs allowed for reproducible production of size-controlled nanoparticles that have a long shelf life, and these constructions may also be functionalized with antigens of various molecular families. Although we did not perform any direct imaging or Dectin-1 knockout studies, both in vitro and in vivo data showed that these AuNPs can generate distinct and powerful immune responses, strongly suggesting that these particles can be endocytosed by APCs and presented to T-cells to produce mature antibodies and helper T-cells. The preliminary data shown here on the quality, magnitude, and uniqueness of the immune response are very encouraging. First, the antibody response was quite respectable for a simple nanoparticle system and compares well with other TACA-based vaccine antibody titers that were generated from either the fully synthetic platforms of Boons et al.,[87,88] the Q-beta-based platforms of the Huang lab,[34] or the MUC4 glycopeptide tetanus toxoid conjugates of the Kunz group.[89] The work from Kunz et al. is most relevant to the present work, as this is the only other group that has used MUC4 tandem repeat TACA-containing glycopeptide units in their work. They report titers of 50,000−400,000 for two vaccinations, which is very comparable to that observed in the present study; in addition, IgG2 is the predominant isotype of the antibodies produced in the present study. Here, we also report results on the cytokine profiles that were generated by presentation of antigen to T-cells by what we assume is an MHC-II-mediated process. Expressions of IL-1β, IL-5, IL-6, interferon-γ, IL-17, IL-21, IL-23, and MIP3α were observed in the cytokine array, indicating a mixed Th1/Th2/Th17 profile (see Table 1). The expression

Table 1. Secreted Cytokine Amounts (in picograms) Detected in Sera of Mice Vaccinated with our MUC4 Glycopeptide B13G Gold Nanoparticle or a Conjugate of That Same Glycopeptide with CRM197

	vaccination epitope			
	B13G-TF-Ser(5)-MUC4-AuNP/SAS	TF-Ser(5)-MUC4-CRM	B13G-AuNP	PBS
cytokine detected	amount (pg)			
IL-1β	271	3806	5	0
IL-5	192	3121	13	7
IL-6	308	4245	14	0
IL-17	14	162	3	2
IL-21	38	0	0	0
IL-23	2912	19304	448	89
INF-γ	485	5367	52	12
MIP1α	11	181	1	11
IL-10	0	0	0	0
TGF-βa	0	71000	0	0

levels of IL-21 are important because it is known to stimulate levels of NK/NKT and $CD8^+$ cells that have proven to be essential in killing certain tumors[90−92] as well as viral-infected cells.[93−95] The lack of both IL-10 and TGF-β expression was also noteworthy as both of these cytokines can have immune-suppressive effects and hence promote tumor expansion. It is important to point out that, in recent years, IL-10 has paradoxically been shown to have antitumor effects depending on the CD8+ T-cell status of the tumor microenvironment.[96] It remains to be seen in future work if the cytokine profile can be adjusted based on vaccine design and what the effect that adjustment may have on therapeutic outcome. Nonetheless, the profiles were similar for both the peptide and the glycopeptide vaccinations, and the antibody responses were

https://doi.org/10.1021/acsbiomedchemau.1c00021
ACS Bio Med Chem Au 2021, 1, 31−43

highly specific for our MUC4 constructs, much as the mAb produced by standard KLH conjugate in a prelude to the present study.[45]

The data from the cytokine array suggest that the CRM-197 conjugates elicit the expression of high circulating levels of cytokines compared to that of the B13G-AuNP (Table 1). However, from ELISpot analysis, when CD4+ T-cells and DCs were stimulated with MUC4, there was an 8-fold increase in quantifiable spots for IFN-y and IL-17 for B13G conjugates compared to CRM-197. When stimulated with TF-Ser(5)-MUC4, there was a reduction in CD4+ activation in comparison to MUC4 stimulation, but the B13G conjugate demonstrated a 4-fold increase of cytokine stimulation. The decrease in CD4+ stimulation toward the glycopeptide can be attributed to possible reduced lysosomal processing of a modified (glycosylated) peptide or lower affinity for the CD4+ T-cell receptor to the antigen-MHC-II complex due to "interference" from the disaccharide. These data bode well for use of simple and widely available materials to construct a vaccine that will raise proper immune responses and whose formulation does not involve the use of detoxified[83] proteins or large multi-epitope-containing carrier molecules[19] that can redirect and dampen the immune response to a chosen immunogen.

The synthesis of the B13G-AuNPs is very simple and modular. It is important to note that this procedure was more efficient under microwave conditions. This is possibly due to maintenance of solubility of the yeast B13G during the reduction or an acceleration of the rate of reaction to facilitate Au^{3+} to Au^{0} reduction and nanoparticle growth seeding.[97] While it is well-known that naked AuNPs as well as citrate-stabilized particles are quite sensitive to aggregation/flocculation under various conditions, passivation with appropriate entities can stabilize AuNPs to a variety of conditions, allowing for use in relative "harsh" milieus (i.e., human serum).[98,99] The success of any AuNP therapy is contingent on this inherent or instilled stability, and our particles have fit this first and critical criterion. Many reports have shown that polysaccharides can act as reducing/coating agents in the synthesis of AuNPs.[100] The use of gums such as gellan,[70] karaya,[68] and katira[69] have been used in what are considered "green" syntheses of AuNPs, where reactive reductants and additional stabilizers are unnecessary. There has been one report of the synthesis of both gold and silver nanoparticles using B13G as the reductant and passivating agent.[65] In this study, Curdlan, which is a linear (no 1,6 branching) B13G produced as an exopolysaccharide from certain Rhizobeaceae species,[101] was used as well as microwave catalysis; however, no biological data were reported, and the quality and size of the particles differed from those presented here.

In addition, B13G are known to form self-assembled nanoparticles, and these have unique applications in the biomedical field.[64,102,103] Some of these particulate forms of B13G have also been used to stabilize nanoparticles for macrophage targeting.[64] In fact, there are many forms of B13G from various sources that have been used in research toward immunological enhancement for some time. B13G are found primarily in yeast and other fungal species as well as in oats, barley, and other cereals and are made up of β-1,3-glucose linkages with various β-1,6 branching points (fungal), whereas the cereal glucans have both β-1,3 and β-1,4 linkages. Curdlan is a linear B13G found in bacteria that has been used in a variety of physical and biochemical studies. Laminarin is a seaweed-derived B13G made up of about a 3:1 ratio of 1,3 and 1,6 linkages.[104] All of these variants have in some form been explored as immune-stimulating entities. Targeting through B13G has been shown to enhance the vaccination efficacy of polysaccharide antigens in antibacterial vaccine design.[49,105] B13G can also assume a variety of structural forms depending on experimental conditions.[72−74,76,77,106] Interestingly, B13G can adopt a triple helix conformation which is relevant to the interaction of this polysaccharide and cellular receptors like Dectin-1.[107] While not completely characterized in the present work, it can be assumed that the B13G on the AuNP surface adopt a conformation that allows proper interaction with Dectin-1 for signal transduction and endocytosis. The processing of the B13G before attaching to AuNPs involved dissolution in base and microwave heating to affect reduction and AuNP formation. While this protocol may unravel a tertiary structural element such as a triple helix, reconstitution of a bioactive conformation is assumed to be facilitated by the "bottom-up" synthesis of self-assembled three-dimensional gold nanospheres. Structural and conformational studies of the on-particle B13G molecules and the relationship these elements have on activity are currently in progress.

In conclusion, we have prepared a robust and simple platform that can target APCs with various families of antigens for antibody production and T-cell activation in a mouse. The simple conjugation and delivery of glycopeptide antigens is highly relevant, as the design of novel therapies based on TACA-containing tandem repeat sequences from tumor-associated mucins is still a very active area of tumor vaccine research; however, no viable products have yet advanced past the various stages of clinical evaluation. The use of a nontoxic, gold nanoparticle platform, combined with pathogen-associated molecular patterns that recognize innate PRRs on APCs, is an approach that potentially can solve many of the issues associated with vaccine constructs designed to date. The ability to deliver relevant antigens through simple peptide and linker chemistry is also an advantage to the current method. The combination of chemoenzymatic TACA synthesis and simple conjugation techniques will allow for the delivery of many different glycopeptide-type antigens with the potential for true immunotherapy against specific cancers. Work toward defining the actual antitumor activity of our platforms against specific pancreatic tumor models is currently underway and will be presented in due course.

EXPERIMENTAL SECTION

General Experimental Procedures

Routine chemicals were purchased from Sigma-Aldrich. Tetrachloroauric acid ($HAuCl_4$) was purchase from Wuhan Golden Wing Industry & Trade Co., Wuhan, China. All amino acids and peptide synthesis materials were purchased from CEM Corp. (Matthews, NC). Peracetylated TF-serine glycoamino acid was either prepared as previously described or purchased from Sussex Research, Ottawa, Ontario, Canada. Solvents were dried in a Grubb still percolation system under a nitrogen atmosphere. MALDI mass spectra were collected on a Shimadzu Axima Confidence MALDI-TOF mass spectrometer equipped a high mass CovalX HM4 detector operated in linear positive ion mode. Samples were prepared for MALDI analysis by desalting using a 0.5 mL 30K Amicon Ultra centrifugal filter. Samples were spotted on an Axima 384-well sample plate using the overlayer method with sinapinic acid as the matrix. Dynamic light scattering and zeta-potential data were collected on a Malvern Nano-ZS Zetasizer instrument. Proton and carbon NMR data were collected

https://doi.org/10.1021/acsbiomedchemau.1c00021
ACS Bio Med Chem Au 2021, 1, 31−43

on either a Bruker NanoBay 400 MHz spectrometer with a Bruker 2-channel SMART probe or on a Bruker AVANCE III 500 MHz spectrometer with a TCI (^{1}H, ^{13}C, ^{15}N) cryoprobe at 25 °C. Most data were run in 90%/10% H_2O/D_2O. Water suppression was performed using excitation sculpting (1D pulse sequence zgesgp). Analytical purity of all compounds was determined by a combination of high-resolution NMR and mass spectrometry data, along with high-performance liquid chromatography. From the combination of these techniques, purity was determined to be >95%.

Peptide/Glycopeptide Synthesis

Peptides sequences were synthesized using a Liberty Prime automated microwave peptide synthesizer (CEM Corp., Matthews, NC, USA). A Rink amide resin (loading 0.6 mmol/g) was used as the solid support. Standard couplings of amino acids were carried out at 0.125 M in dimethylformamide (DMF) using DIC/OxymaPure activation and the corresponding Fmoc-protected amino acid (the synthesis method used is optimized by this activator according to Liberty Prime recommended operation by CEM). Fmoc removal was performed with 40% pyrrolidine in DMF. Coupling of the peracetylated TF-serine glycoamino acid was performed manually at room temperature for 18 h using HOAt, HATU, and 2,4,6-trimethyl pyridine.[71] After glycoamino acid coupling, the resin-bound peptides were added back to the peptide synthesizer, and the sequence was completed per the initial synthesis, except for the addition of DIEA (0.4 equiv) in a 0.25 M solution of OxymaPure in DMF. This modification is also recommended by the manufacturer to buffer the acidity of the Oxyma solution to prevent glycoside hydrolysis. The linker shown in Figure 1 was attached to the N-terminus on-resin using our previously described chemistry.[37,45] Peptides were cleaved from the resin using trifluoroacetic acid (TFA) under gentle agitation over a period of 2 h at 25 °C in the presence of scavengers (TFA/triisopropyl silane/water/DOT (92.5:2.5:2.5:2.5) to avoid oxidation. The majority of TFA was removed by a stream of nitrogen, and the crude peptides were precipitated by the addition of ice-cold diethyl ether. The precipitates were centrifuged, dried, and purified by high-performance liquid chromatography on reverse-phase C18 columns using specific gradients of water and acetonitrile (solvents A and B), each containing 0.1% TFA. Characterization was by high-resolution mass spectrometry and high-resolution NMR.

Synthesis and Characterization of B13G-AuNPs

β-1,3(1−6)-Glucan (yeast beta-glucan, Megazyme, Bray, Ireland; 3 mg) was suspended in 4.9 mL of Milli-Q H_2O containing 100 μL of 1 M NaOH. This suspension was heated to 90 °C for 30 min in a Biotage Initiator microwave reactor to fully dissolve the β-1,3-glucan. A portion of this B13G stock solution (1.67 mL) was diluted with 3.11 mL of H_2O and 67 μL of 1 M NaOH. This mixture was heated to 90 °C for 5 min in the microwave reactor. After this initial heating, 100 μL of 10 mM $HAuCl_4$ was introduced into the mixture. The mixture was then microwave-heated to 90 °C for 60 min to form the β-1,3-glucan AuNPs. The final concentrations of reagents were β-1,3-glucan (1 mg/mL), $HAuCl_4$ (0.1 mg/mL), NaOH (20 mM). β-1,3-Glucan AuNPs were isolated by centrifugation on 50 kDa MWCO centricon filters at 4000 rpm for 10 min. The particles were diluted with water repeatedly washed in this manner (7×), further diluted with water, and passed through a 0.45 μm filter. The particles were analyzed by UV/vis (IMPLEN nanophotometer NP80), DLS (Malvern Zetasizer Nano-ZS), and carbohydrate analysis (vide supra and Supporting Information).

The place exchange reaction to add the linker-conjugated peptide and glycopeptide to the particle was performed by dissolving 1 mg of either MUC4-PEG-SH or TF-Ser(5)-MUC4-PEG-SH in 1 mL of water and mixing with 3 mL of the freshly prepared B13G-AuNPs in a glass vial. The reaction was placed in a shaking incubator overnight at 45 °C. Ultrafiltration of residual small molecules was affected by ultrafiltration using 50K MW cutoff spin filters. Filtration was repeated seven times and washed with Ultrapure Milli-Q water at each step.

Mouse Immunizations

In vivo studies were performed according to the Frederick National Laboratory for Cancer Research (Frederick, MD) Animal Care and Use Committee (ACUC) guidelines. Frederick National Laboratory is accredited by AAALAC International and follows the Public Health Service Policy for the Care and Use of Laboratory Animals. Animal care was provided in accordance with the procedures outlined in the "Guide for Care and Use of Laboratory Animals" (National Research Council; 2011; National Academies Press; Washington, DC). Pathogen-free C57BL/6 female mice age 6−10 weeks were purchased from Charles River Laboratories International, Inc. (Frederick, MD).

Immunizations were performed on sets of five mice per group. Animals were injected on days 0, 14, 28, and 42 by intraperitoneal injection with 30 μg of nanoparticles (B13G-AuNPs, B13G-MUC4-AuNPs, or B13G-MUC4-Ser(5)-AuNPs) in 100 μL of buffer solution with addition of either 100 μL of Sigma Adjuvant System or TiterMax Gold Adjuvants or 1× PBS for control. On day 52, blood serum was obtained via cardiac puncture, and the spleens were harvested. The spleens were pooled and homogenized from each of the experimental and control groups. Mouse CD4+, CD8+, and DCs were isolated from each of the groups via MojoSortTM isolation kits. The isolated cells were then used in ELISpot assays.

Similar to the protocol above, vaccinations with a TF-MUC4-CRM197 conjugate were performed in a similar manner only this time using 3 μg of the this 7 conjugate in 100 μL of 1× PBS (pH 7.4) along with 100 μL of SAS. On day 52, blood sera and spleens were processed as described above.

■ ASSOCIATED CONTENT

Supporting Information

The Supporting Information is available free of charge at https://pubs.acs.org/doi/10.1021/acsbiomedchemau.1c00021.

TEM, DLS, and zeta-potential data, nanoparticle stability studies, cytokine responses, ELISpot images, and mass spectrometry and NMR characterization data (PDF)

■ AUTHOR INFORMATION

Corresponding Author

Joseph J. Barchi, Jr. − *Chemical Biology Laboratory, Center for Cancer Research, National Cancer Institute at Frederick, Frederick, Maryland 21702, United States;* orcid.org/0000-0001-9906-0799; Email: barchij@mail.nih.gov

Authors

Kevin R. Trabbic − *Chemical Biology Laboratory, Center for Cancer Research, National Cancer Institute at Frederick, Frederick, Maryland 21702, United States*

Kristopher A. Kleski − *Chemical Biology Laboratory, Center for Cancer Research, National Cancer Institute at Frederick, Frederick, Maryland 21702, United States*

Complete contact information is available at: https://pubs.acs.org/10.1021/acsbiomedchemau.1c00021

Author Contributions

K.R.T. conceived the project and designed and performed most of the experiments; K.A.K. helped with experiment optimization and performed stability studies; J.J.B. conceived the project, designed, and oversaw all experiments and wrote the paper.

Notes

The authors declare no competing financial interest.

https://doi.org/10.1021/acsbiomedchemau.1c00021
ACS Bio Med Chem Au 2021, 1, 31−43

ACKNOWLEDGMENTS

We thank James Kelley of the CBL for help with high-resolution mass spectra, and Kunio Nagashima and the Electron Microscopy Laboratory, Frederick National Laboratories, for TEM images. This project has been funded in whole or in part with federal funds from the National Cancer Institute, National Institutes of Health, under Contract No. HHSN261200800001E. The content of this publication does not necessarily reflect the views or policies of the Department of Health and Human Services, nor does mention of trade names, commercial products, or organizations imply endorsement by the U.S. Government.

REFERENCES

(1) Hakomori, S. I. New Directions in Cancer-Therapy Based on Aberrant Expression of Glycosphingolipids - Antiadhesion and Ortho-Signaling Therapy. *Cancer Cell-Mon Rev.* **1991**, *3* (12), 461−470.
(2) Feizi, T.; Childs, R. A. Carbohydrate Structures of Glycoproteins and Glycolipids as Differentiation Antigens, Tumor-Associated Antigens and Components of Receptor Systems. *Trends Biochem. Sci.* **1985**, *10* (1), 24−29.
(3) Dabelsteen, E. Cell surface carbohydrates as prognostic markers in human carcinomas. *J. Pathol.* **1996**, *179* (4), 358−369.
(4) Andreana, P. R. Zwitterionic polysaccharide (PS A1) as an immune elicitor for vaccine development. *Abstr. Pap. Am. Chem. S* **2009**, *237*, 748−748.
(5) Jin, K. T.; Lan, H. R.; Chen, X. Y.; Wang, S. B.; Ying, X. J.; Lin, Y.; Mou, X. Z. Recent advances in carbohydrate-based cancer vaccines. *Biotechnol. Lett.* **2019**, *41* (6−7), 641−650.
(6) Wei, M. M.; Wang, Y. S.; Ye, X. S. Carbohydrate-based vaccines for oncotherapy. *Med. Res. Rev.* **2018**, *38* (3), 1003−1026.
(7) Feng, D. Y.; Shaikh, A. S.; Wang, F. S. Recent Advance in Tumor-associated Carbohydrate Antigens (TACAs)-based Antitumor Vaccines. *ACS Chem. Biol.* **2016**, *11* (4), 850−863.
(8) Amon, R.; Reuven, E. M.; Leviatan Ben-Arye, S.; Padler-Karavani, V. Glycans in immune recognition and response. *Carbohydr. Res.* **2014**, *389*, 115−122.
(9) Liu, C. C.; Ye, X. S. Carbohydrate-based cancer vaccines: target cancer with sugar bullets. *Glycoconjugate J.* **2012**, *29* (5−6), 259−271.
(10) Yin, Z. J.; Huang, X. F. Recent Development in Carbohydrate Based Anticancer Vaccines. *J. Carbohydr. Chem.* **2012**, *31* (1−3), 143−186.
(11) Guo, Z. W.; Wang, Q. L. Recent development in carbohydrate-based cancer vaccines. *Curr. Opin. Chem. Biol.* **2009**, *13* (5−6), 608−617.
(12) Franco, A. Glycoconjugates as vaccines for cancer immunotherapy: Clinical trials and future directions. *Anti-Cancer Agents Med. Chem.* **2008**, *8* (1), 86−91.
(13) Xu, Y.; Sette, A.; Sidney, J.; Gendler, S. J.; Franco, A. Tumor-associated carbohydrate antigens: a possible avenue for cancer prevention. *Immunol. Cell Biol.* **2005**, *83* (4), 440−8.
(14) Toyokuni, T.; Singhal, A. K. Synthetic Carbohydrate Vaccines Based on Tumor-Associated Antigens. *Chem. Soc. Rev.* **1995**, *24* (4), 231−242.
(15) Yang, Z. G.; Ma, Y. F.; Zhao, H.; Yuan, Y.; Kim, B. Y. S. Nanotechnology platforms for cancer immunotherapy. *Wiley Interdiscip. Rev.: Nanomed. Nanobiotechnol.* **2020**, *12* (2), e1590.
(16) Hu, J.; Wei, P.; Seeberger, P. H.; Yin, J. Mannose-Functionalized Nanoscaffolds for Targeted Delivery in Biomedical Applications. *Chem. - Asian J.* **2018**, *13* (22), 3448−3459.
(17) Yin, Z.; Wu, X.; Kaczanowska, K.; Sungsuwan, S.; Comellas Aragones, M.; Pett, C.; Yu, J.; Baniel, C.; Westerlind, U.; Finn, M.G.; Huang, X. Antitumor Humoral and T Cell Responses by Mucin-1 Conjugates of Bacteriophage Q beta in Wild-type Mice. *ACS Chem. Biol.* **2018**, *13* (6), 1668−1676.
(18) Yin, Z. J.; Comellas-Aragones, M.; Chowdhury, S.; Bentley, P.; Kaczanowska, K.; BenMohamed, L.; Gildersleeve, J. C.; Finn, M. G.; Huang, X. F. Boosting Immunity to Small Tumor-Associated Carbohydrates with Bacteriophage Q beta Capsids. *ACS Chem. Biol.* **2013**, *8* (6), 1253−1262.
(19) Buskas, T.; Thompson, P.; Boons, G. J. Immunotherapy for cancer: synthetic carbohydrate-based vaccines. *Chem. Commun.* **2009**, No. 36, 5335−5349.
(20) Thompson, P.; Lakshminarayanan, V.; Supekar, N. T.; Bradley, J. M.; Cohen, P. A.; Wolfert, M. A.; Gendler, S. J.; Boons, G. J. Linear synthesis and immunological properties of a fully synthetic vaccine candidate containing a sialylated MUC1 glycopeptide. *Chem. Commun.* **2015**, *51* (50), 10214−10217.
(21) Tagliamonte, M.; Petrizzo, A.; Tornesello, M. L.; Buonaguro, F. M.; Buonaguro, L. Antigen-specific vaccines for cancer treatment. *Hum. Vaccines Immunother.* **2014**, *10* (11), 3332−3346.
(22) Pietersz, G. A.; Pouniotis, D. S.; Apostolopoulos, V. Design of Peptide-Based Vaccines for Cancer. *Frontiers in Medicinal Chemistry*; Bentham Science Publishers, 2010; Vol. *5*, pp 127−166.
(23) Pietersz, G. A.; Pouniotis, D. S.; Apostolopoulos, V. Design of peptide-based vaccines for cancer. *Curr. Med. Chem.* **2006**, *13* (14), 1591−1607.
(24) Ingale, S.; Wolfert, M. A.; Buskas, T.; Boons, G. J. Increasing the Antigenicity of Synthetic Tumor-Associated Carbohydrate Antigens by Targeting Toll-Like Receptors. *ChemBioChem* **2009**, *10* (3), 455−463.
(25) Zhou, Z. F.; Lin, H.; Li, C.; Wu, Z. M. Recent progress of fully synthetic carbohydrate-based vaccine using TLR agonist as build-in adjuvant. *Chin. Chem. Lett.* **2018**, *29* (1), 19−26.
(26) Nishat, S.; Andreana, P. R. Entirely Carbohydrate-Based Vaccines: An Emerging Field for Specific and Selective Immune Responses. *Vaccines* **2016**, *4* (2), 19.
(27) Krishnamachari, Y.; Geary, S. M.; Lemke, C. D.; Salem, A. K. Nanoparticle Delivery Systems in Cancer Vaccines. *Pharm. Res.* **2011**, *28* (2), 215−236.
(28) Zhang, Y.; Lin, S. B.; Wang, X. Y.; Zhu, G. Z. Nanovaccines for cancer immunotherapy. *Wiley Interdiscip. Rev.: Nanomed. Nanobiotechnol.* **2019**, *11* (5), e1559.
(29) Sun, Z. Y.; Chen, P. G.; Liu, Y. F.; Zhang, B. D.; Wu, J. J.; Chen, Y. X.; Zhao, Y. F.; Li, Y. M. Multi-component self-assembled anti-tumor nano-vaccines based on MUC1 glycopeptides. *Chem. Commun.* **2016**, *52* (48), 7572−7575.
(30) Teran-Navarro, H.; Calderon-Gonzalez, R.; Salcines-Cuevas, D.; Garcia, I.; Marradi, M.; Freire, J.; Salmon, E.; Portillo-Gonzalez, M.; Frande-Cabanes, E.; Garcia-Castano, A.; Martinez-Callejo, V.; Gomez-Roman, J.; Tobes, R.; Rivera, F.; Yanez-Diaz, S.; Alvarez-Dominguez, C. Pre-clinical development of Listeria-based nano-vaccines as immunotherapies for solid tumours: insights from melanoma. *Oncoimmunology* **2019**, *8* (2), e1541534.
(31) Calderon-Gonzalez, R.; Teran-Navarro, H.; Garcia, I.; Marradi, M.; Salcines-Cuevas, D.; Yanez-Diaz, S.; Solis-Angulo, A.; Frande-Cabanes, E.; Farinas, M. C.; Garcia-Castano, A.; Gomez-Roman, J.; Penades, S.; Rivera, F.; Freire, J.; Alvarez-Dominguez, C. Gold glyconanoparticles coupled to listeriolysin O 91−99 peptide serve as adjuvant therapy against melanoma. *Nanoscale* **2017**, *9* (30), 10721−10732.
(32) Parry, A. L.; Clemson, N. A.; Ellis, J.; Bernhard, S. S. R.; Davis, B. G.; Cameron, N. R. 'Multicopy Multivalent' Glycopolymer-Stabilized Gold Nanoparticles as Potential Synthetic Cancer Vaccines. *J. Am. Chem. Soc.* **2013**, *135* (25), 9362−9365.
(33) Salahuddin, N.; Elbarbary, A. A.; Salem, M. L.; Elksass, S. Antimicrobial and antitumor activities of 1,2,4-triazoles/polypyrrole chitosan core shell nanoparticles. *J. Phys. Org. Chem.* **2017**, *30* (12), e3702.
(34) Sungsuwan, S.; Wu, X. J.; Huang, X. F. Evaluation of Virus-Like ParticleBased Tumor-Associated Carbohydrate Immunogen in a Mouse Tumor Model. *Methods Enzymol.* **2017**, *597*, 359−376.
(35) Yin, Z. J.; Dulaney, S.; Mckay, C. S.; Baniel, C.; Kaczanowska, K.; Ramadan, S.; Finn, M. G.; Huang, X. F. Chemical Synthesis of GM2 Glycans, Bioconjugation with Bacteriophage Q beta, and the

https://doi.org/10.1021/acsbiomedchemau.1c00021
ACS Bio Med Chem Au 2021, 1, 31−43

Induction of Anticancer Antibodies. *ChemBioChem* **2016**, *17* (2), 174−180.
(36) Gibadullin, R.; Farnsworth, D. W.; Barchi, J. J.; Gildersleeve, J. C. GalNAc-Tyrosine Is a Ligand of Plant Lectins, Antibodies, and Human and Murine Macrophage Galactose-Type Lectins. *ACS Chem. Biol.* **2017**, *12* (8), 2172−2182.
(37) Brinas, R. P.; Sundgren, A.; Sahoo, P.; Morey, S.; Rittenhouse-Olson, K.; Wilding, G. E.; Deng, W.; Barchi, J. J., Jr. Design and synthesis of multifunctional gold nanoparticles bearing tumor-associated glycopeptide antigens as potential cancer vaccines. *Bioconjugate Chem.* **2012**, *23* (8), 1513−1523.
(38) Svarovsky, S. A.; Szekely, Z.; Barchi, J. J. Synthesis of gold nanoparticles bearing the Thomsen-Friedenreich disaccharide: a new multivalent presentation of an important tumor antigen. *Tetrahedron: Asymmetry* **2005**, *16* (2), 587−598.
(39) Biswas, S.; Medina, S. H.; Barchi, J. J. Synthesis and cell-selective antitumor properties of amino acid conjugated tumor-associated carbohydrate antigen-coated gold nanoparticles. *Carbohydr. Res.* **2015**, *405*, 93−101.
(40) Glinskii, O. V.; Li, F.; Wilson, L. S.; Barnes, S.; Rittenhouse-Olson, K.; Barchi, J. J.; Pienta, K. J.; Glinsky, V. V. Endothelial integrin alpha 3 beta 1 stabilizes carbohydrate-mediated tumor/endothelial cell adhesion and induces macromolecular signaling complex formation at the endothelial cell membrane. *Oncotarget* **2014**, *5* (5), 1382−1389.
(41) Sundgren, A.; Barchi, J. J. Varied presentation of the Thomsen-Friedenreich disaccharide tumor-associated carbohydrate antigen on gold nanoparticles. *Carbohydr. Res.* **2008**, *343* (10−11), 1594−1604.
(42) Gautam, S. K.; Kumar, S.; Cannon, A.; Hall, B.; Bhatia, R.; Nasser, M. W.; Mahapatra, S.; Batra, S. K.; Jain, M. MUC4 mucin- a therapeutic target for pancreatic ductal adenocarcinoma. *Expert Opin. Ther. Targets* **2017**, *21* (7), 657−669.
(43) Kurtenkov, O.; Innos, K.; Sergejev, B.; Klaamas, K. The Thomsen-Friedenreich Antigen-Specific Antibody Signatures in Patients with Breast Cancer. *BioMed Res. Int.* **2018**, *2018*, 1.
(44) Almogren, A.; Abdullah, J.; Ghapure, K.; Ferguson, K.; Glinsky, V. V.; Rittenhouse-Olson, K. Anti-Thomsen-Friedenreich-Ag (anti-TF-Ag) potential for cancer therapy. *Front. Biosci., Scholar Ed.* **2012**, *S4* (3), 840−863.
(45) Trabbic, K. R.; Whalen, K.; Abarca-Heideman, K.; Xia, L.; Temme, J. S.; Edmondson, E. F.; Gildersleeve, J. C.; Barchi, J. J. A Tumor-Selective Monoclonal Antibody from Immunization with a Tumor-Associated Mucin Glycopeptide. *Sci. Rep.* **2019**, *9* (1), 5662.
(46) Janeway, C. A.; Medzhitov, R. Innate immune recognition. *Annu. Rev. Immunol.* **2002**, *20*, 197−216.
(47) Bauer, S.; Muller, T.; Hamm, S. Pattern Recognition by Toll-Like Receptors. *Adv. Exp. Med. Biol.* **2009**, *653*, 15−34.
(48) Kaisho, T.; Akira, S. Toll-like receptor function and signaling. *J. Allergy Clin. Immunol.* **2006**, *117* (5), 979−987.
(49) Mayer, S.; Raulf, M. K.; Lepenies, B. C-type lectins: their network and roles in pathogen recognition and immunity. *Histochem. Cell Biol.* **2017**, *147* (2), 223−237.
(50) Penades, S.; de la Fuente, J. M.; Barrientos, A. G.; Clavel, C.; Martinez-Avila, O.; Alcantara, D. Multifunctional glyconanoparticles: Applications in biology and biomedicine. *Nanomaterials for Application in Medicine and Biology*; NATO Science for Peace and Security Series B: Physics and Biophysics; Springer: Dordrecht, The Netherlands, 2008; pp 93−101.
(51) Gauthier, L.; Chevallet, M.; Bulteau, F.; Thepaut, M.; Delangle, P.; Fieschi, F.; Vives, C.; Texier, I.; Deniaud, A.; Gateau, C. Lectin recognition and hepatocyte endocytosis of GalNAc-decorated nanostructured lipid carriers. *J. Drug Target* **2021**, *29* (1), 99−107.
(52) Kleski, K. A.; Trabbic, K. R.; Shi, M. C.; Bourgault, J. P.; Andreana, P. R. Enhanced Immune Response Against the Thomsen-Friedenreich Tumor Antigen Using a Bivalent Entirely Carbohydrate Conjugate. *Molecules* **2020**, *25* (6), 1319.
(53) Napoletano, C.; Zizzari, I. G.; Rughetti, A.; Rahimi, H.; Irimura, T.; Clausen, H.; Wandall, H. H.; Belleudi, F.; Bellati, F.; Pierelli, L.; Frati, L.; Nuti, M. Targeting of macrophage galactose-type C-type lectin (MGL) induces DC signaling and activation. *Eur. J. Immunol.* **2012**, *42* (4), 936−945.
(54) Nuti, M.; Zizzari, I.; Napoletano, C.; Rughetti, A.; Rahimi, H.; Antonilli, M.; Bellati, F.; Di Costanzo, F.; Irimura, T.; Wandall, H.; Clausen, H.; Benedetti Panici, P. Macrophage galactose-type C-type lectin receptor for DC targeting of antitumor glycopeptide vaccines. *J. Clin. Oncol.* **2011**, *29* (15), e13528.
(55) Bundle, D. R.; Paszkiewicz, E.; Elsaidi, H. R. H.; Mandal, S. S.; Sarkar, S. A Three Component Synthetic Vaccine Containing a beta-Mannan T-Cell Peptide Epitope and a beta-Glucan Dendritic Cell Ligand. *Molecules* **2018**, *23* (8), 1961.
(56) Decout, A.; Silva-Gomes, S.; Drocourt, D.; Blattes, E.; Riviere, M.; Prandi, J.; Larrouy-Maumus, G.; Caminade, A. M.; Hamasur, B.; Kallenius, G.; Kaur, D.; Dobos, K. M.; Lucas, M.; Sutcliffe, I. C.; Besra, G. S.; Appelmelk, B. J.; Gilleron, M.; Jackson, M.; Vercellone, A.; Tiraby, G.; Nigou, J. Deciphering the molecular basis of mycobacteria and lipoglycan recognition by the C-type lectin Dectin-2. *Sci. Rep.* **2018**, *8*, 16840.
(57) Xie, J. H.; Guo, L.; Ruan, Y. Y.; Zhu, H. Y.; Wang, L.; Zhou, L.; Yun, X. J.; Gu, J. X. Laminarin-mediated targeting to Dectin-1 enhances antigen-specific immune responses. *Biochem. Biophys. Res. Commun.* **2010**, *391* (1), 958−962.
(58) Backer, R.; van Leeuwen, F.; Kraal, G.; den Haan, J. M. M. CD8(−) dendritic cells preferentially cross-present Saccharomyces cerevisiae antigens. *Eur. J. Immunol.* **2008**, *38* (2), 370−380.
(59) De Marco Castro, E.; Calder, P. C.; Roche, H. M. beta-1,3/1,6-Glucans and Immunity: State of the Art and Future Directions. *Mol. Nutr. Food Res.* **2021**, *65* (1), 1901071.
(60) Nasrollahzadeh, M.; Shafiei, N.; Nezafat, Z.; Soheili Bidgoli, N. S.; Soleimani, F. Recent progresses in the application of cellulose, starch, alginate, gum, pectin, chitin and chitosan based (nano)-catalysts in sustainable and selective oxidation reactions: A review. *Carbohydr. Polym.* **2020**, *241*, 116353.
(61) Devi, L.; Gupta, R.; Jain, S. K.; Singh, S.; Kesharwani, P. Synthesis, characterization and in vitro assessment of colloidal gold nanoparticles of Gemcitabine with natural polysaccharides for treatment of breast cancer. *J. Drug Delivery Sci. Technol.* **2020**, *56*, 101565.
(62) Padil, V. V. T.; Waclawek, S.; Cernik, M.; Varma, R. S. Tree gum-based renewable materials: Sustainable applications in nanotechnology, biomedical and environmental fields. *Biotechnol. Adv.* **2018**, *36* (7), 1984−2016.
(63) Devendiran, R. M.; Chinnaiyan, S. K.; Yadav, N. K.; Moorthy, G. K.; Ramanathan, G.; Singaravelu, S.; Sivagnanam, U. T.; Perumal, P. T. Green synthesis of folic acid-conjugated gold nanoparticles with pectin as reducing/stabilizing agent for cancer theranostics. *RSC Adv.* **2016**, *6* (35), 29757−29768.
(64) Soto, E.; Ostroff, G. Glucan Particles as Carriers of Nanoparticles for Macrophage-Targeted Delivery. *ACS Symp. Ser.* **2012**, *1119*, 57−79.
(65) El-Naggar, M. E.; Shaheen, T. I.; Fouda, M. M. G.; Hebeish, A. A. Eco-friendly microwave-assisted green and rapid synthesis of well-stabilized gold and core-shell silver-gold nanoparticles. *Carbohydr. Polym.* **2016**, *136*, 1128−1136.
(66) Palma, A. S.; Feizi, T.; Zhang, Y. B.; Stoll, M. S.; Lawson, A. M.; Diaz-Rodriguez, E.; Campanero-Rhodes, M. A.; Costa, J.; Gordon, S.; Brown, G. D.; Chai, W. G. Ligands for the beta-glucan receptor, Dectin-1, assigned using "designer" microarrays of oligosaccharide probes (neoglycolipids) generated from glucan polysaccharides. *J. Biol. Chem.* **2006**, *281* (9), 5771−5779.
(67) Sze, D. M. Y.; Chan, G. C. F. Effects of Beta-Glucans on Different Immune Cell Populations and Cancers. *Adv. Bot. Res.* **2012**, *62*, 179−196.
(68) Gangapuram, B. R.; Bandi, R.; Dadigala, R.; Kotu, G. M.; Guttena, V. Facile Green Synthesis of Gold Nanoparticles with Carboxymethyl Gum Karaya, Selective and Sensitive Colorimetric Detection of Copper (II) Ions. *J. Cluster Sci.* **2017**, *28* (5), 2873−2890.

https://doi.org/10.1021/acsbiomedchemau.1c00021
ACS Bio Med Chem Au 2021, 1, 31−43

(69) Maity, S.; Kumar Sen, I.; Sirajul Islam, S. Green synthesis of gold nanoparticles using gum polysaccharide of Cochlospermum religiosum (katira gum) and study of catalytic activity. *Phys. E* **2012**, *45*, 130−134.
(70) Dhar, S.; Mali, V.; Bodhankar, S.; Shiras, A.; Prasad, B. L. V.; Pokharkar, V. Biocompatible gellan gum-reduced gold nanoparticles: cellular uptake and subacute oral toxicity studies. *J. Appl. Toxicol.* **2011**, *31* (5), 411−420.
(71) Zhang, Y. L.; Muthana, S. M.; Farnsworth, D.; Ludek, O.; Adams, K.; Barchi, J. J.; Gildersleeve, J. C. Enhanced Epimerization of Glycosylated Amino Acids During Solid-Phase Peptide Synthesis. *J. Am. Chem. Soc.* **2012**, *134* (14), 6316−6325.
(72) Sletmoen, M.; Stokke, B. T. Review: Higher order structure of (1,3)-beta-D-glucans and its influence on their biological activities and complexation abilities. *Biopolymers* **2008**, *89* (4), 310−321.
(73) Okobira, T.; Miyoshi, K.; Uezu, K.; Sakurai, K.; Shinkai, S. Molecular dynamics studies of side chain effect on the beta-1,3-D-glucan triple helix in aqueous solution. *Biomacromolecules* **2008**, *9* (3), 783−788.
(74) Yadomae, T. Structure and biological activities of fungal beta-1,3-glucans. *Yakugaku Zasshi* **2000**, *120* (5), 413−431.
(75) McIntire, T. M.; Brant, D. A. Observations of the (1 -> 3)-beta-D-glucan linear triple helix to macrocycle interconversion using noncontact atomic force microscopy. *J. Am. Chem. Soc.* **1998**, *120* (28), 6909−6919.
(76) Bohn, J. A.; BeMiller, J. N. 1->3)-beta-D-glucans as biological response modifiers: A review of structure-functional activity relationships. *Carbohydr. Polym.* **1995**, *28* (1), 3−14.
(77) Saito, H.; Tabeta, R.; Yoshioka, Y.; Hara, C.; Kiho, T.; Ukai, S. A High-Resolution Solid-State C-13 Nmr-Study of the Secondary Structure of Branched (1−3)-Beta-D-Glucans from Fungi - Evidence of 2 Kinds of Conformers, Curdlan-Type Single-Helix and Laminaran-Type Triple-Helix Forms, as Manifested from the Conformation-Dependent C-13 Chemical-Shifts. *Bull. Chem. Soc. Jpn.* **1987**, *60* (12), 4267−4272.
(78) Pooja, D.; Panyaram, S.; Kulhari, H.; Reddy, B.; Rachamalla, S. S.; Sistla, R. Natural polysaccharide functionalized gold nanoparticles as biocompatible drug delivery carrier. *Int. J. Biol. Macromol.* **2015**, *80*, 48−56.
(79) Kim, T.; Lee, K.; Gong, M. S.; Joo, S. W. Control of gold nanoparticle aggregates by manipulation of interparticle interaction. *Langmuir* **2005**, *21* (21), 9524−9528.
(80) Burgi, T. Properties of the gold-sulphur interface: from self-assembled monolayers to clusters. *Nanoscale* **2015**, *7* (38), 15553−15567.
(81) MacCalman, T. E.; Phillips-Jones, M. K.; Harding, S. E. Glycoconjugate vaccines: some observations on carrier and production methods. *Biotechnol. Genet. Eng. Rev.* **2019**, *35* (2), 93−125.
(82) Dagan, R.; Poolman, J.; Siegrist, C. A. Glycoconjugate vaccines and immune interference: A review. *Vaccine* **2010**, *28* (34), 5513−23.
(83) Hsieh, C. L. Characterization of saccharide-CRM197 conjugate vaccines. *Dev Biol. (Basel)* **2000**, *103*, 93−104.
(84) Mittal, S. K.; Cho, K. J.; Ishido, S.; Roche, P. A. Interleukin 10 (IL-10)-mediated Immunosuppression: MARCH-I INDUCTION REGULATES ANTIGEN PRESENTATION BY MACROPHAGES BUT NOT DENDRITIC CELLS. *J. Biol. Chem.* **2015**, *290* (45), 27158−27167.
(85) Mittal, S. K.; Roche, P. A. Suppression of antigen presentation by IL-10. *Curr. Opin. Immunol.* **2015**, *34*, 22−27.
(86) Soares, K. C.; Rucki, A. A.; Kim, V.; Foley, K.; Solt, S.; Wolfgang, C. L.; Jaffee, E. M.; Zheng, L. TGF-beta blockade depletes T regulatory cells from metastatic pancreatic tumors in a vaccine dependent manner. *Oncotarget* **2015**, *6* (40), 43005−43015.
(87) Ingale, S.; Wolfert, M. A; Gaekwad, J.; Buskas, T.; Boons, G.-J. Robust immune responses elicited by a fully synthetic three-component vaccine. *Nat. Chem. Biol.* **2007**, *3* (10), 663−667.
(88) Buskas, T.; Ingale, S.; Boons, G. J. Towards a fully synthetic carbohydrate-based anticancer vaccine: Synthesis and immunological evaluation of a lipidated glycopeptide containing the tumor-associated Tn antigen. *Angew. Chem., Int. Ed.* **2005**, *44* (37), 5985−5988.
(89) Cai, H.; Palitzsch, B.; Hartmann, S.; Stergiou, N.; Kunz, H.; Schmitt, E.; Westerlind, U. Antibody induction directed against the tumor-associated MUC4 glycoprotein. *ChemBioChem* **2015**, *16* (6), 959−67.
(90) Davis, M. R.; Zhu, Z. W.; Hansen, D. M.; Bai, Q.; Fang, Y. J. The role of IL-21 in immunity and cancer. *Cancer Lett.* **2015**, *358* (2), 107−114.
(91) Thedrez, A.; Harly, C.; Morice, A.; Salot, S.; Bonneville, M.; Scotet, E. IL-21-Mediated Potentiation of Antitumor Cytolytic and Proinflammatory Responses of Human V gamma 9V delta 2 T Cells for Adoptive Immunotherapy. *J. Immunol.* **2009**, *182* (6), 3423−3431.
(92) Davis, I. D.; Skak, K.; Hunder, N.; Smyth, M. J.; Sivakumar, P. V. Interleukin-21 and Cancer Therapy. *Targeted Cancer Immune Therapy* **2009**, 43−59.
(93) Mendez-Lagares, G.; Lu, D.; Merriam, D.; Baker, C. A.; Villinger, F.; Van Rompay, K. K. A.; McCune, J. M.; Hartigan-O'Connor, D. J. IL-21 Therapy Controls Immune Activation and Maintains Antiviral CD8(+) T Cell Responses in Acute Simian Immunodeficiency Virus Infection. *AIDS Res. Hum. Retroviruses* **2017**, *33*, S81−S92.
(94) Pallikkuth, S.; Parmigiani, A.; Pahwa, S. The role of interleukin-21 in HIV infection. *Cytokine Growth Factor Rev.* **2012**, *23* (4−5), 173−180.
(95) Sarra, M.; Pallone, F.; Macdonald, T. T.; Monteleone, G. Targeting Interleukin-21 in Immune-Mediated Pathologies. *Curr. Drug Targets* **2010**, *11* (5), 645−649.
(96) Qiao, J.; Liu, Z. D.; Dong, C. B.; Luan, Y.; Zhang, A. L.; Moore, C.; Fu, K.; Peng, J. J.; Wang, Y.; Ren, Z. H.; Han, C. H.; Xu, T.; Fu, Y. X. Targeting Tumors with IL-10 Prevents Dendritic Cell-Mediated CD8(+) T Cell Apoptosis. *Cancer Cell* **2019**, *35* (6), 901−915.e4.
(97) Li-Ping, Y.; Wei-Xia, T. Studies on Au colloidal nanoparticles synthesized by microwave irradiation. *Wuli Huaxue Xuebao* **2006**, *22* (4), 513−516.
(98) Mukhopadhyay, A.; Grabinski, C.; Afrooz, A. R. M. N.; Saleh, N. B.; Hussain, S. Effect of Gold Nanosphere Surface Chemistry on Protein Adsorption and Cell Uptake In Vitro. *Appl. Biochem. Biotechnol.* **2012**, *167* (2), 327−337.
(99) Daniel, M. C.; Astruc, D. Gold nanoparticles: Assembly, supramolecular chemistry, quantum-size-related properties, and applications toward biology, catalysis, and nanotechnology. *Chem. Rev.* **2004**, *104* (1), 293−346.
(100) Escarcega-Gonzalez, C. E.; Garza-Cervantes, J. A.; Vazquez-Rodriguez, A.; Morones-Ramirez, J. R. Bacterial Exopolysaccharides as Reducing and/or Stabilizing Agents during Synthesis of Metal Nanoparticles with Biomedical Applications. *Int. J. Polym. Sci.* **2018**, *2018*, 1.
(101) Cai, Z. X.; Zhang, H. B. Recent progress on Curdlan provided by functionalization strategies. *Food Hydrocolloids* **2017**, *68*, 128−135.
(102) Liu, Q. Y.; Duan, B. C.; Xu, X. J.; Zhang, L. N. Progress in rigid polysaccharide-based nanocomposites with therapeutic functions. *J. Mater. Chem. B* **2017**, *5* (29), 5690−5713.
(103) Sakurai, K.; Uezu, K.; Numata, M.; Hasegawa, T.; Li, C.; Kaneko, K.; Shinkai, S. beta-1,3-glucan polysaccharides as novel one-dimensional hosts for DNA/RNA, conjugated polymers and nanoparticles. *Chem. Commun.* **2005**, No. 35, 4383−4398.
(104) Okazaki, M.; Adachi, Y.; Ohno, N.; Yadomae, T. Structure-Activity Relationship of (1-]3)-Beta-D-Glucans in the Induction of Cytokine Production from Macrophages, in-Vitro. *Biol. Pharm. Bull.* **1995**, *18* (10), 1320−1327.
(105) Qiao, W. L.; Ji, S. Y.; Zhao, Y. B.; Hu, T. Conjugation of beta-glucan markedly increase the immunogencity of meningococcal group Y polysaccharide conjugate vaccine. *Vaccine* **2015**, *33* (17), 2066−2072.
(106) Yoshioka, Y.; Uehara, N.; Saito, H. Conformation-Dependent Change in Antitumor-Activity of Linear and Branched (1−3)-Beta-D-Glucans on the Basis of Conformational Elucidation by C-13 Nuclear-

Magnetic-Resonance Spectroscopy. *Chem. Pharm. Bull.* **1992**, *40* (5), 1221−1226.
(107) Hanashima, S.; Ikeda, A.; Tanaka, H.; Adachi, Y.; Ohno, N.; Takahashi, T.; Yamaguchi, Y. NMR study of short beta(1−3)-glucans provides insights into the structure and interaction with Dectin-1. *Glycoconjugate J.* **2014**, *31* (3), 199−207.

https://doi.org/10.1021/acsbiomedchemau.1c00021
ACS Bio Med Chem Au 2021, 1, 31−43